Separation of Enantiomers and Racemate Formation in Two-Dimensional Crystals at the Water Surface from Racemic α-Amino Acid Amphiphiles: Design and Structure

Isabelle Weissbuch,*,† Maria Berfeld,† Wim Bouwman,‡ Kristian Kjaer,‡ Jens Als-Nielsen,§ Meir Lahav,*,† and Leslie Leiserowitz*,†

Contribution from the Department of Materials & Interfaces, The Weizmann Institute of Science, 76100 Rehovot, Israel, Department of Solid State Physics, Risø National Laboratory, DK 4000, Roskilde, Denmark, and Niels Bohr Institute, H. C. Ørsted Laboratory, DK 2100, Copenhagen, Denmark

Received April 29, 1996. Revised Manuscript Received November 27, 1996[⊗]

Abstract: Studies are presented on the two-dimensional (2-D) crystalline packing arrangements of enantiomerically pure and racemic α-amino acid $RHC(NH_3^+)CO_2^-$ monolayers on water and on glycine aqueous solutions, as determined by synchrotron grazing incidence X-ray diffraction. The amphiphiles have been designed such that their racemic mixtures form 2-D crystals which are either heterochiral (for $R = C_nH_{2n+1}-$, $n = 10, 12, 16$) due to the tendency for herringbone chain arrangements via glide symmetry or homochiral (for $R = C_nH_{2n+1}CONH(CH_2)_4-$, $n = 11, 17, 21$) by virtue of hydrogen bonding by translation of the amide group in the chains leading to a spontaneous separation into islands of opposite chirality. The two different crystalline motifs led to a correlation between their packing arrangements and induced oriented nucleation of 3-D crystals of α-glycine by these monolayers. The relevance of the present results to the possibility of ordering and spontaneous segregation of racemates of the natural hydrophobic α-amino acids at the air-solution interface is discussed.

Introduction

The routes by which basic units of living systems, such as the α-amino acids, have adopted only one sense of chirality remains an unsolved mystery of nature.[1] Spontaneous segregation of enantiomers from a racemic mixture might have played an important role in an abiotic process proposed to explain the tranformation from a racemic chemistry to a chiral biology. Thus much focus has been placed on the use of three-dimensional (3-D) crystals for inducing spontaneous resolution of left- and right-handed molecules.[2−6] In two-dimensions, such a separation at interfaces may be no less important. On simple symmetry grounds, it should in fact be easier to bring about a segregation of enantiomers in two-dimensional (2-D) crystalline domains formed by chiral amphiphilic molecules at an air−liquid or air−solid interface, since the inversion symmetry element, so prevalent in 3-D crystals, is absent in the 2-D counterpart. However, the glide symmetry element is still available for packing molecules of opposite handedness in such crystalline monolayers.

Various studies for the detection of chiral segregation of amphiphiles at the air−water interface have been reported.[7−15] Recently, chiral separation in monolayers of racemic myristoylalanine has been inferred from grazing incidence X-ray diffraction.[16] Monolayer domains of mirror-image structures, and therefore of opposite chirality, have been observed on mica support by scanning force microscopy[17] and on graphite by scanning tunneling microscopy.[18]

Natural Hydrophobic α-Amino Acids at the Air-Solution Interface

Several years ago, it was reported that addition of naturally occurring hydrophobic α-amino acids to supersaturated glycine aqueous solutions induced the formation of floating α-glycine crystals which exposed their (010) or ($0\bar{1}0$) faces to air, depending upon whether the absolute configuration of the

† The Weizmann Institute of Science.
‡ Risø National Laboratory.
§ H. C. Ørsted Laboratory.
⊗ Abstract published in *Advance ACS Abstracts,* January 15, 1997.

(1) Pasteur, L. *Ann. Phys.* **1848**, *24*, 442.
(2) Havinga, E. *Biochem. Biophys. Acta* **1954**, *13*, 171.
(3) Wald, G. *N. Y. Acad. Sci.* **1957**, *69*, 352.
(4) Addadi, L.; Lahav, M. In *Origins of Optical Activity in Nature*; Walker, D. C., Ed.; Elsevier: New York, 1979; p 179.
(5) Weissbuch, I.; Addadi, L.; Berkovitch-Yellin, Z.; Gati, E.; Lahav, M.; Leiserowitz, L. *Nature* **1984**, *310*, 161.
(6) Weissbuch, I.; Popovitz-Biro, R.; Leiserowitz, L.; Lahav, M. In *The Lock and-Key Principle*; Behr, J. P., Ed.; John Wiley & Sons Ltd.: 1994; p 173.
(7) Rose, P. L.; Harvey, N. G.; Arnett, E. M. In *Advances in Physical Organic Chemistry*; Academic Press Limited: 1993; Vol. 28, p 45.
(8) Lösche, M.; Sackmann, E.; Möhwald, H. *Ber. Bunsenges. Phys. Chem.* **1983**, *87*, 848.
(9) Weiss, R. M.; McConnell, H. M. *Nature* **1984**, *310*, 47.
(10) Rietz, R.; Brezesinski, G.; Möhwald, H. *Ber. Bunsenges. Phys. Chem.* **1993**, *97*, 1394.
(11) Brezesinski, G.; Rietz, R.; Kjaer, K.; Bouwman, W. G.; Möhwald, H. *Nuovo Cimento D* **1994**, *16*, 1487.
(12) Scalas, E.; Brezesinski, G.; Bouwman, W. G.; Kjaer, K.; Möhwald, H. *Proc. XXX the Rencontres de Moriond* **1995**, 165.
(13) Scalas, E.; Brezesinski, G.; Möhwald, H.; Kaganer, V. M.; Bouwman, W. G.; Kjaer, K., *Thin Solid Films*; **1996**, Proceedings of the LB7 Conference, Ancona, **1996**, *284*/*285*, 56.
(14) Rietz, R.; Rettig, W.; Brezesinski, G.; Bouwman, W. G.; Kjaer, K.; Möhwald, H., *Thin Solid Films*; 1996, Proceedings of the LB7 Conference, Ancona, **1996**, *284*/*285*, 211.
(15) Gehlert, U.; Weidemann, G.; Volhardt, D.; Bringezu, F.; Struth, B.; Scalas, E.; Brezesinski, G.; Möhwald, H. *HASYLAB, DESY, Annual Report*; 1994; p 421.
(16) Nassoy, P.; Goldmann, M.; Bouloussa, O.; Rondelez, F. *Phys. Rev. Lett.* **1995**, *75*, 457.
(17) Echardt, C. J.; Peachey, N. M.; Swanson, D. R.; Takacs, J. M.; Khan, M. A.; Gong, X.; Kim, J.-H.; Wang, J.; Uphaus, R. A. *Nature* **1993**, *362*, 614.
(18) Stevens, F.; Dyer, D. J.; Walba, D. M. *Angew. Chem., Int. Ed. Engl.* **1996**, *35*, 900.

S0002-7863(96)01392-3 CCC: $14.00

additive was (*R*) or (*S*), respectively.[5,19] In 3-D crystals[20−23] these α-amino acids all pack in hydrogen-bonded layers in which the molecules are related only by translation,[24] in arrangements similar to that of the (010) layer of α-glycine[25] (Figure 1a,b). This layer match[26] suggested formation, at the air-aqueous solution interface, of ordered two-dimensional domains of the hydrophobic α-amino acid additives.

Crystallization of α-glycine in the presence of the racemic hydrophobic α-amino acids also yielded floating α-glycine crystals but now exposing both (010) and ($0\bar{1}0$) faces to air in equal proportions.[19] The racemic 3-D crystal structures can be divided into two classes. In one class, which includes branched α-amino acids (*R*,*S*) val,[27] isoleu,[28] and leu,[29] each hydrogen-bonded layer consists of molecules related by translation as in α-glycine (Figure 1a,b). This layer arrangement would be consistent with the formation, at the air-solution interface, of *two-dimensional homochiral domains* of opposite handedness. In the other class, represented by the crystal structures of straight chain α-amino acids (*R*,*S*)-α-aminobutyric acid,[30] met,[31] and norleu,[32] each layer consists of both enantiomers related via glide symmetry (Figure 1c). This would be consistent with the formation, at the air-glycine solution interface, of ordered *two-dimensional heterochiral domains*.

Apart from the α-glycine crystal growth experiments, there is no evidence whether the racemic α-amino acids at the solution surface spontaneously separate into left- and right-handed ordered domains or whether within each domain the two enantiomers are related by glide symmetry.

Design of Synthetic α-Amino Acid Monolayer Templates

Our object was to design synthetic templates of α-amino acid amphiphiles—amenable to study by grazing incidence X-ray diffraction (GID) at the air−water interface[33]—that would form two different types of monolayer arrangements: one in which the molecules in a racemic mixture would be related by glide symmetry, and the other in which the enantiomers separate into islands of opposite chirality. We thus investigated two classes of zwitterionic α-amino acid amphiphiles $RHC(NH_3^+)CO_2^-$.

(i) In one class the α-amino acid residue, R was chosen to be an alkyl chain $C_nH_{2n+1}-$, $n = 10,12,16$, to help induce the herring-bone motif via glide symmetry, as in Figure 1c, (ii) The α-amino acid residue, R in the second class, $C_nH_{2n+1}CONH-(CH_2)_4-$ $n = 11, 17, 21, 29$, contains an amide group, CONH, to promote translational packing (as in Figure 1a) by virtue of a tendency for hydrogen-bonding by 5 Å translation,[39] and so induce segregation of the racemic mixture into enantiomeric domains.

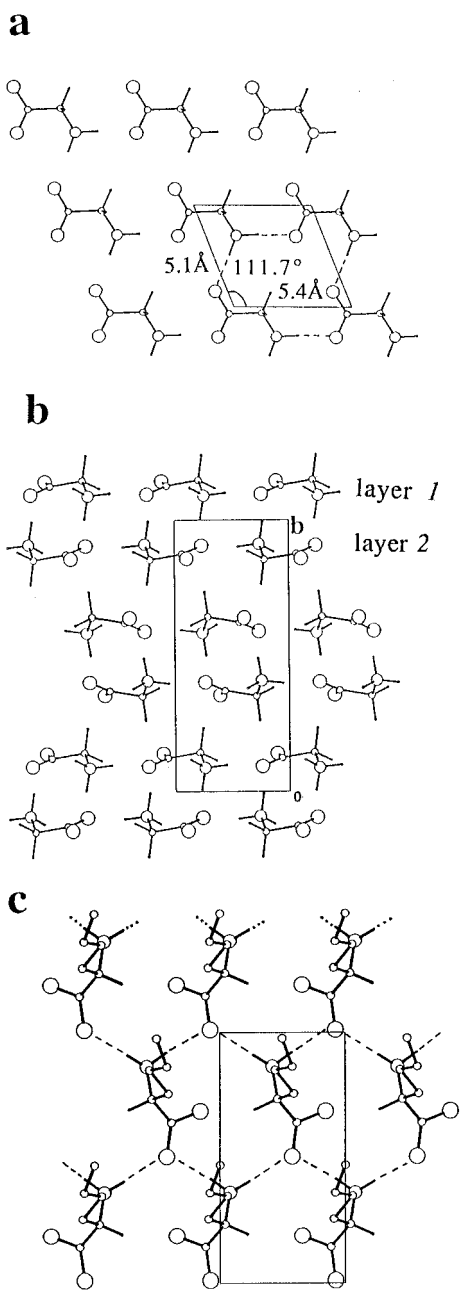

Figure 1. The 3-D crystalline packing arrangement of α-glycine: (a) view perpendicular to the hydrogen-bonded layer and (b) view along the 5.1 Å axis showing the hydrogen-bonded bilayers generated by inversion symmetry. (c) The hydrogen-bonded layer in the 3-D crystal structure of (*R*,*S*)-norleu.

(19) Weissbuch, I.; Addadi, L.; Lahav, M.; Leiserowitz, L. *J. Am. Chem. Soc.* **1988**, *110*, 561−567.
(20) Torii, K.; Iitaka, Y. *Acta Crystallogr.* **1970**, *B26*, 1317.
(21) Torii, K.; Iitaka, Y. *Acta Crystallogr.* **1971**, *B27*, 2237.
(22) Torii, K.; Iitaka, Y. *Acta Crystallogr.* **1973**, *B29*, 2799.
(23) Harding, M. M.; Howieson, R. M. *Acta Crystallogr.* **1976**, *B32*, 2799.
(24) In systems with two independent molecules per asymmetric unit the molecules are related by *pseudo*-translation.
(25) Legros, J.-P.; Kvick, Å. *Acta Crystallogr.* **1980**, *B36*, 3052−3059.
(26) Weissbuch, I.; Frolow, F.; Addadi, L.; Lahav, M.; Leiserowitz, L. *J. Am. Chem. Soc.* **1990**, *112*, 7718.
(27) Mallikarjunan, M.; Rao, S. T. *Acta Crystallogr.* **1969**, *B25*, 296.
(28) Benedetti, E.; Pedone, C.; Sirigu, A. *Acta Crystallogr.* **1973**, *B29* 730.
(29) diBlasio, B.; Pedone, C.; Sirigu, A. *Acta Crystallogr.* **1975**, *B31*, 601.
(30) Nakata, K.; Y. Takaki; Sakurai; K., *Acta Crystallogr.* **1980**, *B36*, 504.
(31) Mathieson, A. M. *Acta Crystallogr.* **1952**, *5*, 332.
(32) Mathieson, A. M. *Acta Crystallogr.* **1953**, *6*, 399.
(33) Such measurements were made several years ago on monolayers of (*R*) N^{ϵ}-palmitoyl lysine;[34] the racemic monolayer did not, however, yield a GID pattern.[35] Recent technical improvements[36−38] led to the present reexamination of such types of α-amino acid molecules.
(34) Wolf, S. G.; Leiserowitz, L.; Lahav, M.; Deutsch, M.; Kjaer, K.; Als-Nielsen, J. *Nature* **1987**, *328*, 63.
(35) Jacquemain, D.; Grayer Wolf, S.; Leveiller, F.; Deutsch, M.; Kjaer, K.; Als-Nielsen, J.; Lahav, M.; Leiserowitz, L. *Angew. Chem., Int. Ed. Engl.* **1992**, *31*, 130.
(36) Als-Nielsen, J.; Jacquemain, D.; Kjaer, K.; Leveiller, F.; Lahav, M.; Leiserowitz, L. *Physics Reports* **1994**, *246*, 251.
(37) Als-Nielsen, J.; Kjaer, K.; Linderholm, J.; Bang, S.; Skaarup, P.; Vogeley, E.; Hansen, E. In *Annual Progress Report of the Department of Solid State Physics 1991*; Als-Nielsen, J., Skov Pedersen, J., Lebech, B., Eds.; Risø National Laboratory: Roskilde, Denmark, 1992; p 10.
(38) Kjaer, K.; Majewski, J.; Schulte-Schrepping, H.; Weigelt, J. In *Annual Progress Report of the Department of Solid State Physics 1992;* Skov Pedersen, J., Lebech, B., Lindgaard, P.-A., Eds.; Risø National Laboratory: Roskilde, Denmark, 1993; p 131.
(39) Bernstein, J.; Etter, M. C.; Leiserowitz, L. In *Structure Correlation*; Bürgi, H. B., Dunitz, H. D., Eds.; VCH: Weinheim, 1994; Vol. 2, p 431.

Here we report on the packing arrangements of the enantiomerically pure and racemic α-amino acid monolayers on water and on glycine aqueous solutions as well as on the oriented crystallization of α-glycine via these monolayers.

Experimental Section

The α-amino acid amphiphiles have been synthesized and their purity assessed according to known procedures.[40] The compounds used in this study are as follows: 1. (*S*)- and (*R*,*S*)-α-aminostearic acid, abbreviated C_{16}-AA, (*R*)- and (*R*,*S*)-α-aminomyristic acid, C_{12}-AA, (*R*,*S*)-α-aminolauric acid, C_{10}-AA, as α-amino acids with *n*-alkyl chains and 2. N^{ϵ}-long chain derivatives of lysine $C_nH_{2n+1}CO^{\epsilon}NH(CH_2)_4CH(NH_3^+)CO_2^-$ abbreviated as C_n-AM, $n = 11$, 17, 21, 29, as the α-amino acids bearing an amide functional group within the chain separated by a spacer of four methylenes from the head group.

The surface pressure-area isotherms for the monolayers of enantiomerically pure and racemic amphiphiles C_n-AA ($n = 12$, 16) and C_n-AM ($n = 11$, 17, 21, 29) spread on water and on glycine aqueous solutions are similar; the isotherms of C_{10}-AA display a very small surface pressure increase indicating formation of an unstable film. The isotherms for the same monolayers on glycine aqueous solutions are more expanded, but they reach the same limiting area per molecule as on water subphase.

Grazing incidence X-ray diffraction (GID) experiments were carried out on the liquid surface diffractometer[36−38] at the synchrotron beamline BW1, DESY, Hamburg.

The C_n-AA samples for the GID experiments were prepared by spreading chloroform/trifluoroacetic acid (v/v ratio of 98:2) solutions (0.5 mM) on water or glycine aqueous solution (14 g/100 mL) subphase, at 8 °C, for a nominal molecular area of 36 Å^2 (i.e. trough area divided by number of molecules deposited). Spreading was followed by a compression of the monolayer to a nominal area per molecule of 26 Å^2, without any increase in surface pressure in the case of the water subphase or an increase till about 8 mN/m in the case of glycine solutions, and further cooling down to 5 °C.

The C_n-AM samples were prepared as described for C_n-AA, and the GID measurements were performed at the nominal area/molecule of 36 Å^2, with surface pressure not exceeding 3 mN/m, except for (*S*)-C_{11}-AM where measurements were made at 18 Å^2 per molecule, with no observable surface pressure.

In a grazing incidence X-ray diffraction (GID) experiment the evanescent wave is diffracted by the lateral 2-D crystalline order fulfilling the Bragg law and giving the in-plane Bragg peaks. There is no restriction on the vertical scattering component, q_z, of the Bragg scattered beam leading to so called Bragg rods. In the geometry using a Soller collimator and a vertical position sensitive detector (PSD) one thus determines the horizontal (q_{xy}) as well as the vertical (q_z) components of the scattering vectors. From the q_{xy} values one determines the unit cell dimensions, and from the intensity distribution along q_z one determines the molecular packing. The Bragg rod intensity profiles, I(q_z), along q_z were derived from the two-dimensional intensity contour maps I(q_{xy}, q_z), by integrating across q_{xy} for each of the Bragg peaks. The GID data was analyzed in terms of coherence length, unit cell dimensions, and plane group determination as well as X-ray structure factor calculations using atomic coordinate models to fit the Bragg rod intensity profiles, as described elsewhere.[41]

Crystallization of α-glycine under Langmuir monolayers was performed by spreading the amphiphile solutions, for a nominal surface coverage of about 90%, over supersaturated aqueous solutions of glycine (4.66 M) in teflon vessels. The floating crystals were isolated and analyzed for their orientation by crystallographic means, as described elsewhere.[42]

(40) Landau, E. M.; Grayer Wolf, S.; Levanon, M.; Leiserowitz, L.; Lahav, M.; Sagiv, J. *J. Am. Chem. Soc.* **1989**, *111*, 1436.

(41) Leveiller, F.; Jacquemain, D.; Leiserowitz, L.; Kjaer, K.; Als-Nielsen, J. *J. Phys. Chem.* **1992**, *96*, 10380.

(42) Weissbuch, I.; Addadi, L.; Berkovitch-Yellin, Z.; Gati, E.; Weinstein, S.; Lahav, M.; Leiserowitz, L. *J. Am. Chem. Soc.* **1983**, *105*, 6613.

Results and Discussion

Two-Dimensional Crystal Structure Determination of α-Amino Acid Amphiphiles with *n*-Alkyl Chain. The GID patterns of the enantiomerically pure and racemic monolayers, on water and on glycine solution, of the first class of amphiphiles $C_nH_{2n+1}HC(NH_3^+)CO_2^-$, labelled C_n-AA, $n = 10,12,16$, are shown in Figure 2. Only the low-order Bragg diffraction peaks are shown; the high-order peaks are listed in Table 1. The GID patterns from the optically pure amphiphiles (Figure 2, *left*) are significantly different from those of their racemic (Figure 2, *right*) counterparts.

First we analyze the data for the monolayers of the enantiomerically pure amphiphiles. The GID pattern of (*S*)- C_{16}-AA (Figure 2a) spread on water, and (*R*)-C_{12}-AA (Figure 2d) spread on glycine solution, each consisting of five Bragg diffraction peaks, yielded an oblique cell of dimensions $a = 4.91$ Å, $b = 5.25$ Å, $\gamma = 112°$. The tilt angle[43] t between the molecular axis and the normal to the liquid surface was calculated from the q_z maxima of the Bragg rod intensity profiles I(q_z). For (*S*)-C_{16}-AA a chain tilt of ∼36°, with the chains lying in planes close to the normal to the *a* axis was obtained (Scheme 1). The film thickness[44] w, calculated from the full width half maximum *FWHM* of the Bragg rod intensity profiles, was determined to be that of a monolayer. The oblique unit cell contains only one molecule and so is compatible with the plane group *p*1 in which the molecules of single chirality are related by translation symmetry only.

The detailed packing arrangement was obtained by fitting, to the measured Bragg rods, intensity profiles based on X-ray structure factors calculated from atomic coordinate models. The calculated intensity profiles for (*S*)-C_{16}-AA were obtained for planar parallel chains, and the zwitterionic α-amino acid head groups linked by hydrogen bonds as in the layer structure of α-glycine shown in Figure 1a. A comparison of the unit cell axes of (*S*)-C_{16}-AA (Table 1) with that of α-glycine (Figure 1a) shows that there are three distinct ways, shown schematically in Figure 4, in which the head groups may be oriented in the cell and yet form acceptable hydrogen-bonding arrangements. The best fit (Figure 3) was obtained for the motif in which the C−C bond of the head group is parallel to the longer axis *b*, as shown in Figure 5.

Next we analyze the data for the racemic systems. The monolayers of the various racemic amphiphiles C_n-AA, $n =$ 10, 12, 16, spread on water (Figure 2b) and on aqueous glycine solution (Figure 2c−f) yielded similar GID patterns. For (*R*,*S*)-C_{16}-AA on water, the two low-order Bragg peaks as well as the high-order ones yielded a rectangular cell of dimensions $a = 4.80$ Å, $b = 9.67$ Å. The molecular chains are tilted[43] by an angle of about 37° from the normal to the liquid surface in the direction of the *b* axis. The rectangular cell of (*R*,*S*)-C_n-AA is very similar in dimension to the layer in the 3-D crystals of (*R*,*S*)-α-amino acids norleu, met, and α-aminobutyric acid (4.7 Å x 9.8 Å, $\gamma = 90°$) in which the molecules are related by glide symmetry. This similarity clearly denotes a herringbone arrangement for the monolayers. Therefore, the monolayer plane group is *p*1*g*1 with all molecular chains tilted along the *b* axis and the glide plane parallel to the tilt direction. The Bragg rod intensity profiles, calculated on the basis of a molecular model constructed from the (*R*,*S*)-norleucine

(43) The direction of the molecular chain axis in the unit cell was derived from the set of equations $\cos \psi_{hk} \tan t = q_z^{\circ}/|q_{hk}|$, where t is the tilt of the chain, q_z° is the position of the maximum along the Bragg rod, and ψ_{hk} is the azimuthal angle between the tilt direction projected onto the *xy* plane and the reciprocal lattice vector q_{hk}. (See: Kjaer, K. *Physica B* **1994**, *198*, 100).

(44) The film thickness w(Å) ≃ 0.9*2π/*FWHM*, the Scherrer formula.

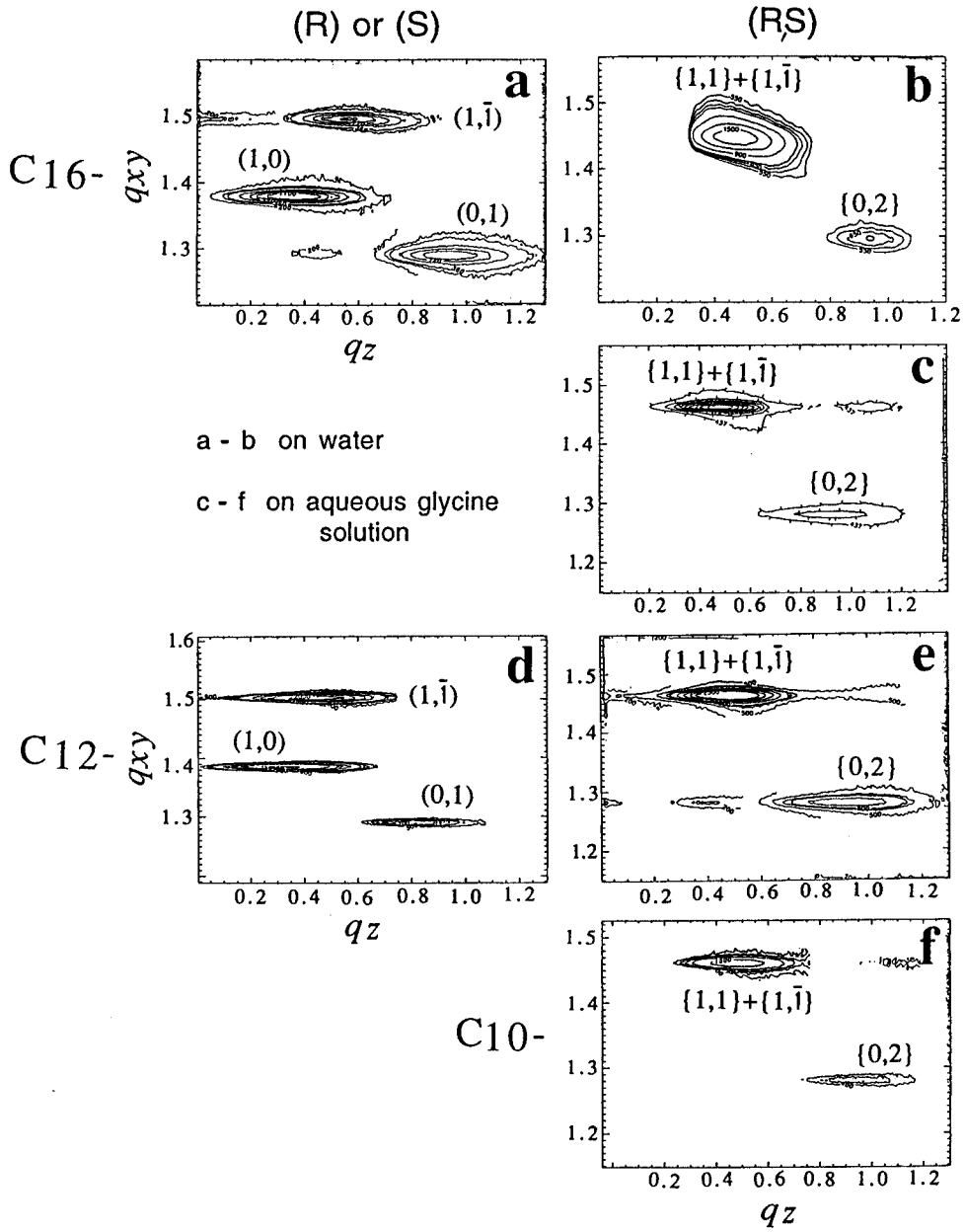

Figure 2. GID patterns from the monolayers of the optically pure and racemic C_n-AA amphiphiles, shown as two-dimensional intensity contour plots $I(q_{xy},q_z)$, along the horizontal q_{xy} and vertical q_z scattering vectors. Monolayers on water subphase: (a) (*S*)-C_{16}-AA and (b) (*R*,*S*)-C_{16}-AA. Monolayers on glycine aqueous solutions: (c) (*R*,*S*)-C_{16}-AA, (d) (*R*)-C_{12}-AA, (e) (*R*,*S*)-C_{12}-AA, and (f) (*R*,*S*)-C_{10}-AA.

Scheme 1

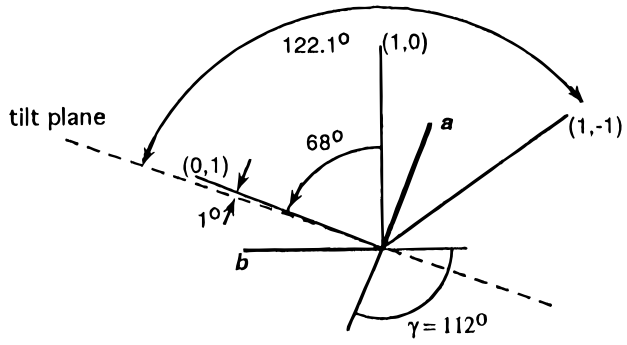

3-D crystal,[32] are shown in Figure 6 for the (*R*,*S*)-C_{16}-AA spread on water. The heterochiral molecular packing arrangement (Figure 7) contains two molecules in the unit cell that are enantiomeric. Each molecule is interlinked by N−H···O-(CO_2^-) hydrogen bonds to two neighboring glide-related molecules.

As alluded to above, the Bragg rod intensity profiles for (*R*,*S*)-C_n-AA spread on glycine aqueous solution are essentially the same in position and shape as on water. But the relative intensities of the different Bragg rods are different. Moreover, the overall intensities of the monolayers spread on glycine solution are stronger. Indeed (*R*,*S*)-C_{10}-AA, which on water gave one very weak Bragg peak, yielded a strong diffraction pattern on glycine solution (Figure 2f). Therefore the addition of glycine to the aqueous subphase enhances crystallinity without perturbing the monolayer structure. The Bragg rod intensity profiles of (*R*,*S*)-C_{16}-AA could be reasonably fitted for about 60−80% coverage of glycine molecules bound to the monolayer head groups by 2-fold screw symmetry parallel to the *a* axis (Figure 8) in an arrangement similar to that observed in the 3-D crystal structures of (*R*,*S*)-norleu, met, and α-aminobutyric acid.

Based on the GID data one can conclude that the racemic mixtures of α-amino acid amphiphiles bearing *n*-alkyl chains spontaneously assemble into heterochiral 2-D crystalline do-

Table 1. Cell Dimensions and Molecular Chain Tilt Angles Derived from the Measured Grazing Incidence X-ray Diffraction Data (q_{hk} and Miller Indexes (hk)) for the Monolayers of $C_nH_{2n+1}CH(NH_3)^+CO_2^-$ n = 10, 12, 16, Spread on Water and on Glycine Aqueous Solutions (14 g/100 mL) at 5 °C

	C_{10}-AA		C_{12}-AA		C_{16}-AA		
	(*R*,*S*)/w	(*R*,*S*)/gly	(*R*)/gly	(*R*,*S*)/gly	(*S*)/w	(*R*,*S*)/w	(*R*,*S*)/gly
a (Å)	*a*	4.76	4.86	4.76	4.91	4.80	4.83
b (Å)		9.74	5.24	9.74	5.25	9.67	9.82
γ (deg)		90	111.6	90	112	90	90
A_m(Å^2)		23.2	23.7	23.2	23.9	23.2	23.7
t (deg)		38	36	35	36	37	37
observed q_{hk} (Å^{-1}) and assigned		1.29;{02}	1.29;{01}	1.29;{02}	1.29;(01)	1.30;{02}	1.28;{02}
(*h*,*k*) of reflection		1.32;{10}[b]	1.39;{10}	1.32;{10}[b]	1.38(10)		1.30;{10}[b]
	1.47;{1$\bar{1}$}	1.46;{11}	1.51;{1$\bar{1}$}	1.47;{11}	1.50;(1$\bar{1}$)	1.45;{11}	1.46;{11}
			2.22;{$\bar{1}$1}		2.21;($\bar{1}$1)	1.83;{12}	
		2.34;{13}	2.59;{$\bar{2}$ 1} +	2.34;{13}	2.57;($\bar{2}$1) +	2.34;{13}	2.32;{13}
		2.64;{20}	{02}	2.64;{20}	(02)	2.62;{20}	2.60;{20}
				2.72;(21)		2.70;{21}	2.67;{21}
plane group		*p*1*g*1	*p*1	*p*1*g*1	*p*1	*p*1*g*1	*p*1*g*1

[a] Only a very weak Bragg peak at q_{xy} = 1.47 Å^{-1} was observed. The peak disappeared during the measurement of the corresponding Bragg rod, presumably because of beam damage. [b] The weak {10} Bragg peak is symmetry permitted in terms of the glide along the *b* axis. The (01) reflection is absent, in keeping with the presence of the glide along *b*.

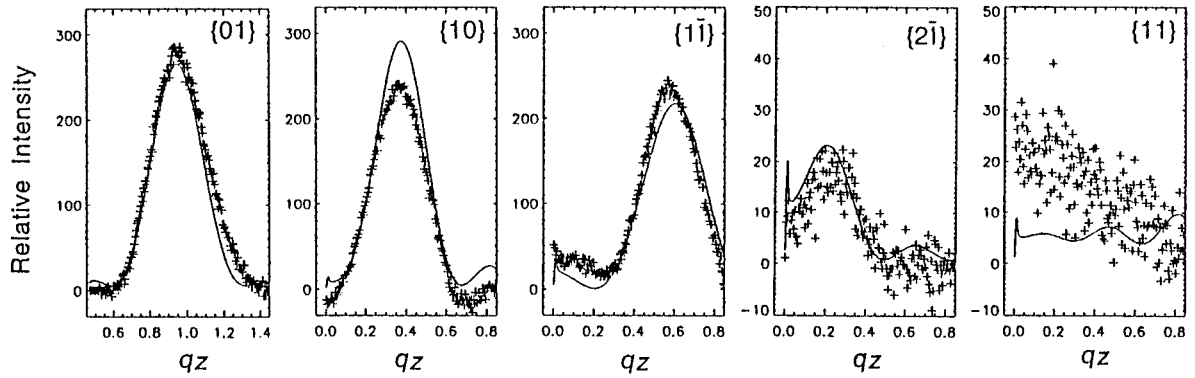

Figure 3. Measured (×) and calculated (—) Bragg rod intensity profiles I(q_z) for the monolayer of (*S*) C_{16}-AA on water subphase. The {0,1}, {1,0}, {1,$\bar{1}$}, {2,$\bar{1}$}, and {1,1} reflections are shown.

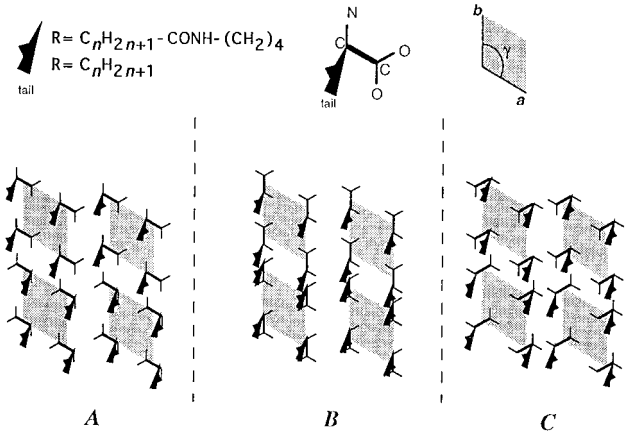

Figure 4. Schematic representation of the possible ways in which the R-HC(NH_3^+)CO_2^- amphiphile molecule is oriented in the unit cell. *A*, *B*, and *C* each represent the two possible orientations (*top* to *bottom*) of the C−C bond of the head group, parallel to the *a*, *b*, and *a* + *b* axes, respectively. For R = $C_nH_{2n+1}CONH(CH_2)_4$−, the chain adopts one of the two possible rotational states (*left* to *right*); for R = C_nH_{2n+1}−, the two rotational states (*left* to *right*) are essentially equivalent.

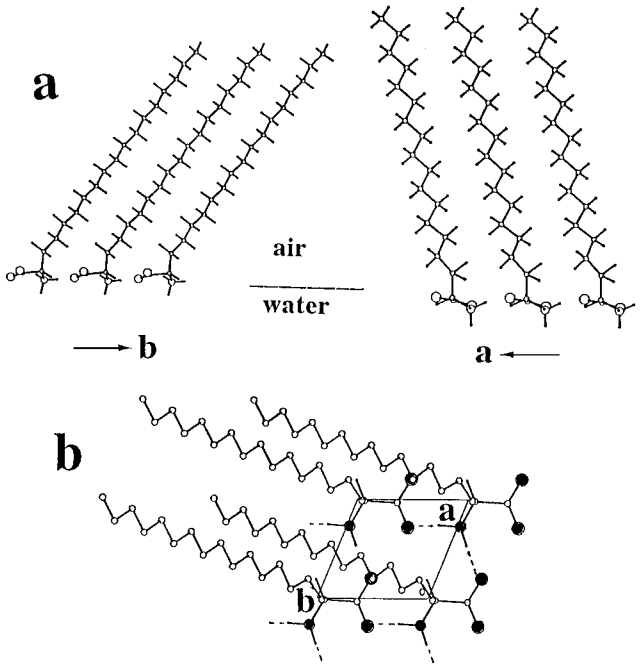

Figure 5. The 2-D crystalline packing arrangement of the (*S*)-C_{16}-AA monolayer on water subphase. Views: (a) parallel and (b) perpendicular to the water surface. For clarity N and O atoms of the head groups in (b) are filled and the H atoms of the *n*-alkyl chains were omitted.

mains in an arrangement similar to the heterochiral layer structure in the 3-D crystals of the short-chain water-soluble counterparts.

Two-Dimensional Crystal Structure Determination of α-Amino Acid Amphiphiles Bearing an Amide Group in the Chain. The GID patterns of the enantiomerically pure and racemic monolayers $C_nH_{2n+1}CONH(CH_2)_4CH(NH_3^+)CO_2^-$, labelled C_n-AM, n = 11, 17, 21, 29, spread on water subphase are shown in Figure 9 (for data summary see Table 2).

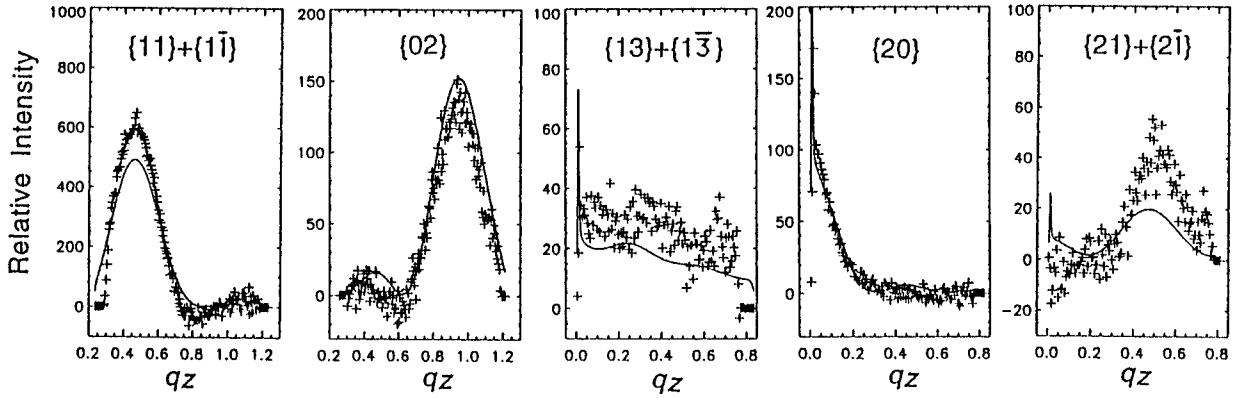

Figure 6. Measured (×) and calculated (—) Bragg rod intensity profiles I(q_z) for the monolayer of (*R,S*)-C_{16}-AA on water. The {1,1} + {1,$\bar{1}$}, {0,2}, {1,3} + {1,3}, {2,0}, and {2,1} + {2,$\bar{1}$} reflections are shown.

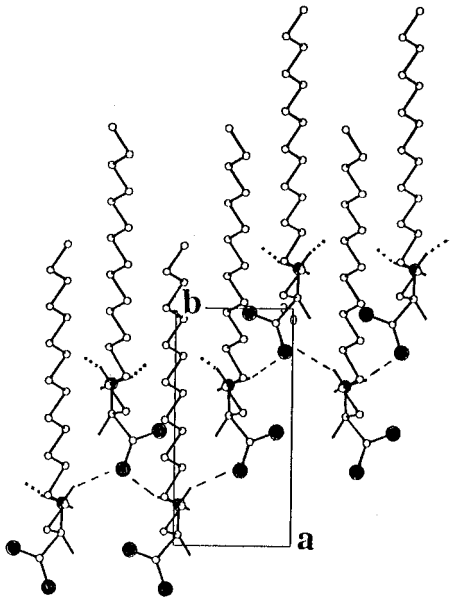

Figure 7. The 2-D crystalline packing arrangement of the heterochiral domains of the (*R,S*)-C_{16}-AA monolayer on water subphase, viewed perpendicular to the layer. For clarity N and O atoms of the head groups are filled and the H atoms of the *n*-alkyl chains were omitted.

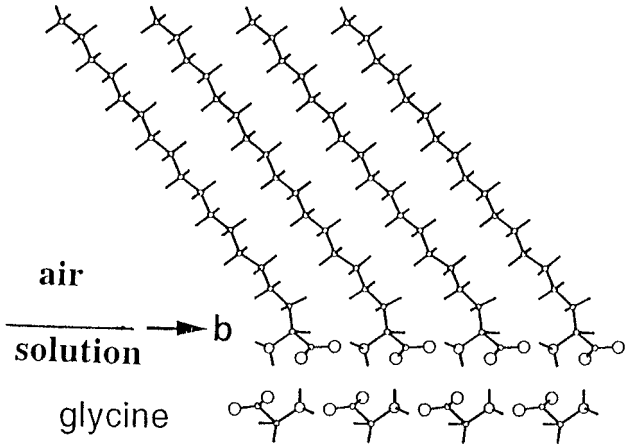

Figure 8. The 2-D crystalline packing arrangement of the heterochiral domains of the (*R,S*)-C_{16}-AA monolayer on glycine aqueous solution. View along the *a* axis showing the C_{16}-AA:glycine heterobilayer generated by the binding of glycine molecules beneath the C_{16}-AA molecules via a pseudo 2-fold screw axis parallel to *a*.

We first present a general interpretation of the GID data of those racemic systems which undergo spontaneous separation into left- and right-handed islands, followed by a detailed analysis of the packing arrangement of (*R,S*)-C_{17}-AM. There is a general similarity between the GID patterns from the films of the three racemic systems (*R,S*)-C_{11}-AM (Figure 9b), (*R,S*)-C_{17}-AM (Figure 9d), and (*R,S*)-C_{21}-AM (Figure 9f) and enantiomerically pure (*S*)-C_{17}-AM (Figure 9c) and (*S*)-C_{21}-AM (Figure 9e), although some of the Bragg peaks of the latter systems are split.[45] The common feature is the presence of three low-order Bragg diffraction peaks at the same q_{xy} and q_z positions, which are also rather similar to the corresponding peaks of the (*S*)-C_{16}-AA (Figure 2a) and (*R*)-C_{12}-AA (Figure 2d). For the (*R,S*)-C_{17}-AM monolayer these three peaks yielded an oblique cell of dimensions $a = 4.92$ Å, $b = 4.98$ Å, $\gamma = 108.5°$ (Table 2), similar in dimensions to that of α-glycine (Figure 1a). The crystalline domains are not very large, with coherence lengths of about 170, 500, and 300 Å, along the (0,1), (1,0), and (1,$\bar{1}$) lattice plane directions, respectively. We derived from the q_z maxima of the three Bragg rod intensity profiles a chain tilt[43] angle of ∼35°, with the chains lying in planes close to the normal to the *a* axis (Scheme 2) and a film thickness[44] consistent with a monolayer. The oblique unit cell of plane group *p*1 contains only one molecule, and, therefore, only translational symmetry is allowed. For these systems not even *pseudo*crystallographic glide symmetry[46] exists within the unit cell, leading to the conclusion that the molecules must be separated into enantiomorphous domains, each of a single chirality.

The detailed packing arrangement of (*R,S*)-C_{17}-AM was obtained by fitting molecular models to the Bragg rod intensity profiles. The molecule was divided into two parts: the α-amino acid head group, $-HC(NH_3^+)CO_2^-$, and the chain $C_{17}H_{35}$-$CONH(CH_2)_4-$. The possible packing arrangements of the head groups must provide hydrogen bonding as in the layer of the 3-D crystal of α-glycine. For each of the possible ways of head group orientation (Figure 4), the chain must be oriented to satisfy the various constraints imposed by interchain contacts, hydrogen bonds between the amide group, and conformational requirements involving chain linkage to the head group. The orientation of the long axis of the hydrocarbon chain is completely determined from the GID data (*vide supra*). Moreover, the plane of the hydrocarbon chain is essentially fixed by the

(45) These split peaks indicate the presence of two to three different yet similar phases, arising presumably from small differences in molecular conformation.

(46) We note that for the monolayer of (*R,S*)-C_n-AM, $n = 21$, the oblique unit cell might be transformed into a centered *pseudo*-rectangular cell $a' = 5.77$ Å, $b' = 8.05$ Å, $\gamma' = 89.5°$, where $a' = a+b$, $b' = b-a$. For $n = 11$ and 17, γ' is 87.4° and 89.3°, respectively. However, the (*R,S*)-C_n-AM monolayers clearly do not have rectangular symmetry. The *pseudo*-rectangular representation of the unit cell of (*R,S*)-C_n-AM is *significantly* different in dimension from the rectangular unit cell of (*R,S*)-C_n-AA ($a = 4.8$ Å, $b = 9.7$ Å). In addition, the molecular chains are tilted in the $2a' + b'$ direction, as opposed to a tilt along the b' axis required by glide symmetry as in the rectangular cell of (*R,S*)-C_n-AA.

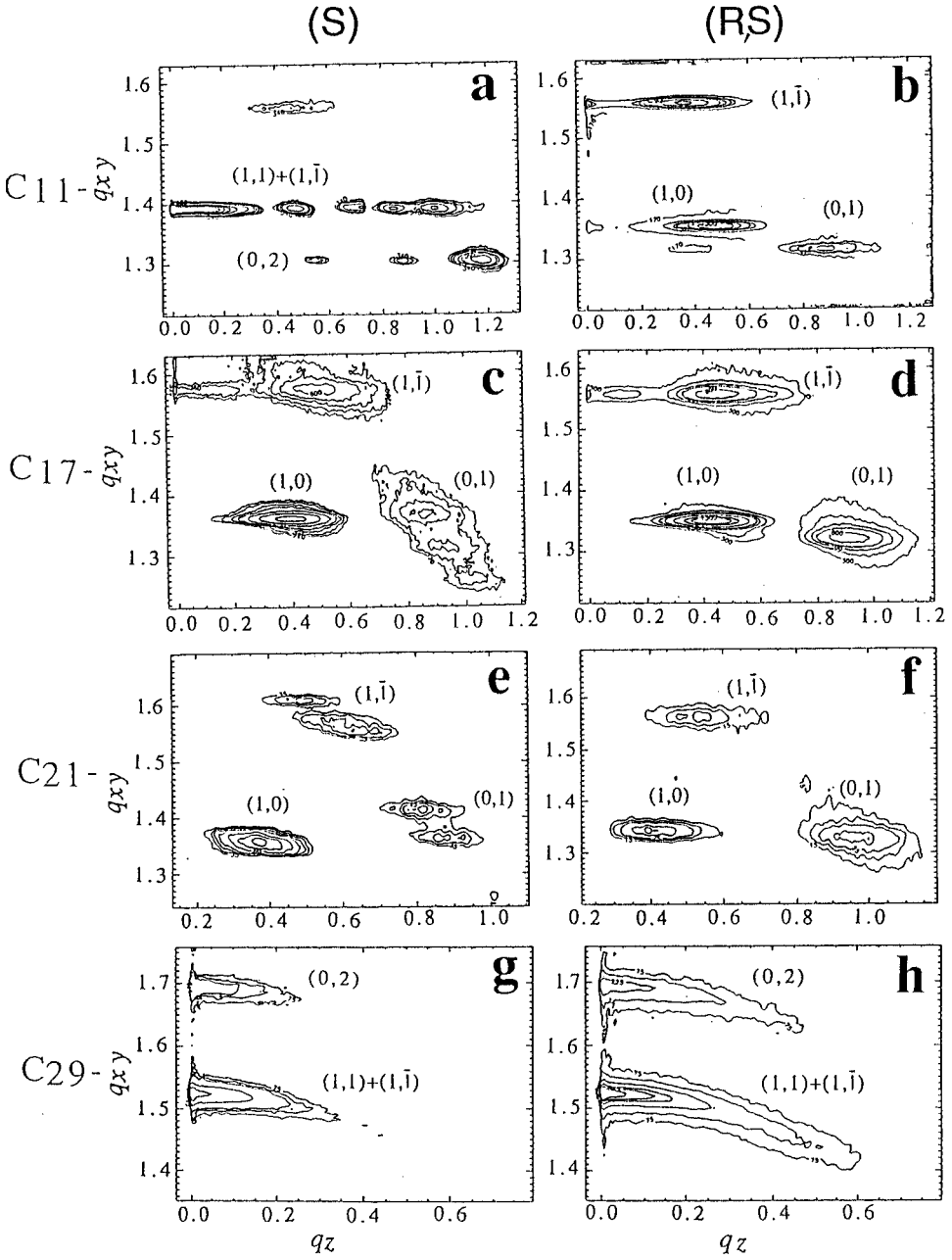

Figure 9. GID patterns from the monolayers of the optically pure and racemic C_n-AM amphiphiles on water surface, shown as two-dimensional intensity contour plots $I(q_{xy},q_z)$, along the horizontal q_{xy} and vertical q_z scattering vectors. (*left*) The (*S*) amphiphiles; (*right*) the (*R,S*) mixtures: (a,b) C_{11}-AM; (c,d) C_{17}-AM; (e,f) C_{21}-AM; (g,h) C_{29}-AM.

tendency for formation of collinear N−H···O═C hydrogen bonds between amide groups related by translation. Thus the chain adopts one of two known rotational states differing by 180°, which are depicted as asymmetric wedges in the left-to-right columns for *A, B, C,* to best satisfy these constraints. There are no more degrees of freedom, resulting in 12 molecular packing models for which we generated Bragg rod profiles. Each of these models was allowed a slight change in molecular conformation to help lower the lattice energy.[47] The two packing arrangements which best satisfied both the hydrogen-bonding requirements and a fit to the observed Bragg rod intensity profiles (Figure 10) are shown in Figure 11 for the molecules of (*R*) configuration. The model in Figure 11b *right* gave a better fit in the shape of the $(1\bar{1})$ Bragg rod and a distinctly lower lattice energy.

(47) CERIUS^2, Molecular Modeling Software for materials research produced by BIOSYM/Molecular Simulations Inc., San Diego, CA and Cambridge, UK.

In conclusion, the racemic monolayers contain enantiomorphous domains composed of molecules of single (*R*) or (*S*) configuration. Naturally, we cannot rule out the presence of a minor amount of enantiomeric disorder. The chiral disorder can occur only via an interchange of the C−H and $C-NH_3^+$ bonds around the asymmetric carbon atom since the hydrocarbon chain must remain in its original position. But it is clear from the two model packing arrangements (Figure 11) that such an interchange, be it random or otherwise, would involve the loss of one hydrogen bond and therefore a decrease in lattice energy of ∼6 kcal/mol.

Of the enantiomerically pure amphiphiles C_n-AM (n = 11,-17,21), the (*S*)-C_{11}-AM is unusual; it yielded a diffraction pattern (Figure 9a) different from that of the (*R,S*) counterpart (Figure 9b). The Bragg peaks yielded a centered rectangular 2-D cell, of dimensions a = 5.1 Å, b = 9.6 Å, very similar to those in the 3-D crystals of the hydrophobic natural α-amino acids such as (*S*)-isoleu[22] and (*S*)-val[21] (5.27 × 9.71 Å). The Bragg rod

Table 2. Cell Dimensions and Molecular Chain Tilt Angles Derived from the Grazing Incidence X-ray Diffraction Data (q_{hk} and Miller Indexes (hk)) for the Monolayers of $C_nH_{2n+1}CONH(CH_2)_4CH(NH_3)^+CO_2^-$, $n = 11, 17, 21, 29$, Spread on Water at 5 °C

	C_{11}-AM		C_{17}-AM		C_{21}-AM		C_{29}-AM	
	(*S*)[a]	(*R*,*S*)	(*S*)[b]	(*R*,*S*)	(*S*)[b]	(*R*,*S*)	(*S*)[c]	(*R*,*S*)
a (Å)	5.10	4.89	4.89	4.92	4.77	4.93	4.94	4.94
b (Å)	9.56	5.02	4.84	4.98	4.94	4.97	7.41	7.40
γ (deg)	90.	109.0	109.8	108.5	111.0	108.8	90	90
A_m(Å^2)	24.4	23.2	22.3	23.2	22.0	23.2	18.3	18.3
t (deg)	40	35	35	35	35	35	0	0
observed q_{hk} (Å^{-1})and assigned (*h*,*k*) of reflection	1.32;{02}	1.32;(01)	1.37;(01)	1.33;(01)	1.41;(01)	1.34;(01)	1.53;(11)	1.52;(11)
	1.40;(1$\bar{1}$)	1.36;(10)	1.36;(10)	1.35;(10)	1.36(10)	1.35;(10)	1.69;(02)	1.70;(02)
	1.40;(1$\bar{1}$)	1.56;(1$\bar{1}$)	1.57;(1$\bar{1}$)	1.57;(1$\bar{1}$)	1.57;(1$\bar{1}$)	1.56;(1$\bar{1}$)	2.54;(20)	2.53(20)
	2.33;(1$\bar{2}$)		2.63;(12)					
	2.33;(12)		2.72;(20)					
	2.63;{04}							

[a] C_{11}-AM forms a multilayer film. [b] The (*S*)-C_{17}-AM and (*S*)-C_{21}-AM monolayers show split Bragg peaks indicating coexistence of phases which differ slightly in their cell dimensions and which could arise from minor differences in chain conformation; therefore, the table gives the values for only one phase. [c] A very weak peak at $q_{xy} = 1.35$ Å^{-1}, corresponding to an unknown minor phase, was also observed.

Scheme 2

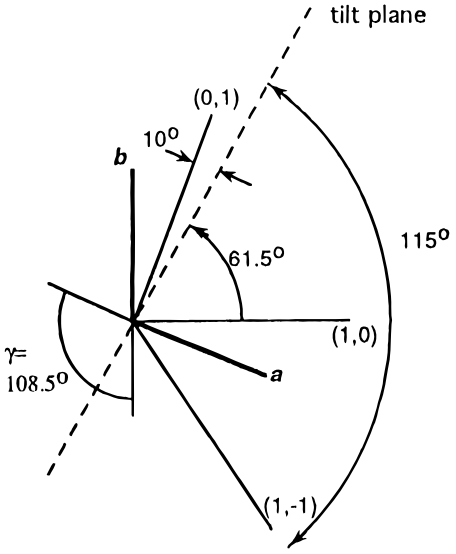

intensity profiles indicate a trilayer[48] formation, explained by the presence of a 2-fold screw axis parallel to the *a* axis which generates a hydrogen-bonded bilayer. The formation of left- and right-handed crystalline monolayer domains from (*R*,*S*)-C_{11}-AM as against trilayer from (*S*)-C_{11}-AM may arise from the dynamics of crystallite growth.

Next we discuss the effect of the predominant contribution of very long hydrocarbon chains on the molecular packing. The GID patterns from the (*S*)- and (*R*,*S*)-C_{29}-AM (Figure 9g,h) monolayers are very similar, but this does not imply for the racemic systems a separation into enantiomorphous territories. The Bragg peaks of each pattern, unlike for the other systems, are skewed denoting that the 2-D crystalline domains deviate from being parallel to the water surface.[49,50] We derived for both systems a rectangular cell of dimensions $a = 4.9$ Å, $b =$ 7.4 Å containing two molecules and thus of molecular area (18.3 Å^2) much lower than that in the other α-amino acid monolayers (Table 2). The cell dimensions and Bragg rod intensity profiles, centered at $q_z \simeq 0$ Å^{-1}, are consistent with chains of the two molecules oriented perpendicular to the *ab* unit cell axes in a herring-bone packing arrangement, implying glide symmetry. For the (*S*)-C_{29}-AM monolayer the unit cell must contain two

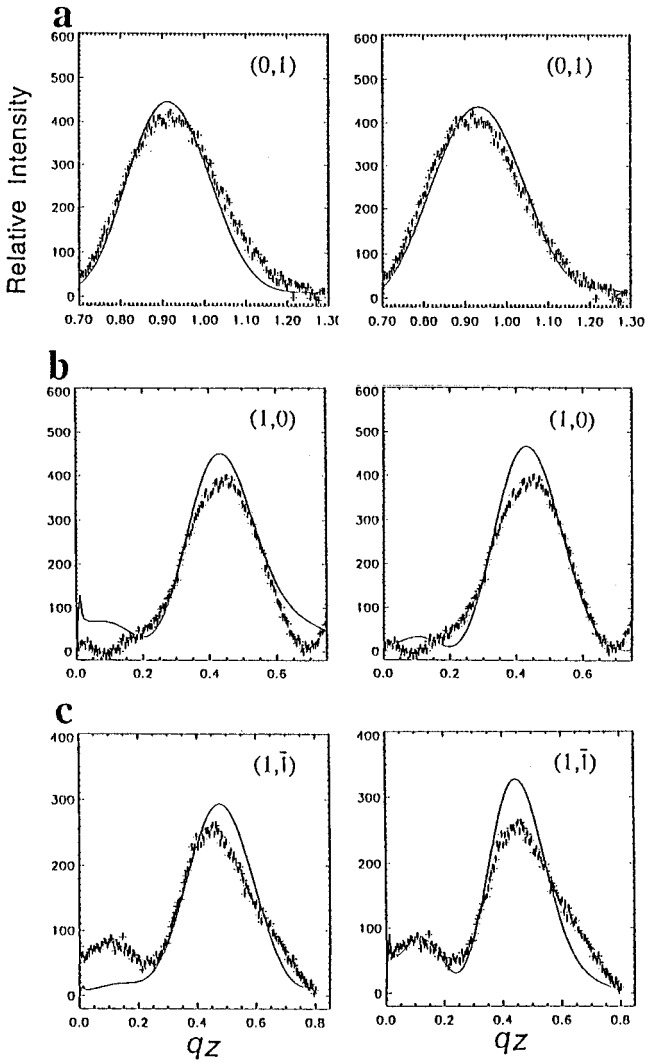

Figure 10. Measured (×) and calculated (—) Bragg rod intensity profiles $I(q_z)$ for the monolayer of (*R*,*S*)-C_{17}-AM on water. The calculated profiles (*left*, *right*) correspond to the two models in Figure 11. (a−c) The (0,1), (1,0), and (1,1̄) reflections.

(48) The Bragg rod intensity profiles display narrow modulations with a *FWHM* of ∼0.13 Å^{-1} corresponding to an average film thickness of 50 Å. The average spacing Δq_z of 0.3 Å^{-1} between the intensity modulations of the Bragg rod at $q_{xy} = 1.32$ Å^{-1} and for some of the modulations at $q_{xy} = 1.40$ Å^{-1}, yields a layer "repeat" distance of ∼20 Å and so a maximum number of three layers (the molecular length is ∼23 Å).

(49) The skewed contours extend along Scherrer rings of constant $q_{tot} = (q_{xy}^2 + q_z^2)^{1/2}$. The skewing was analysed in terms of a mosaic distribution of 2-D crystallites resulting in a film thickness of 45 Å consistent with a monolayer in which the chains are perpendicular to the *ab* unit cell axes.[50]

(50) Kjaer, K.; Bouwman, W. G. In *Annual Progress Report of the Department of Solid State Physics 1994;* Lindgaard, P.-A., Bechgaard, K., Clausen, K. N., Feidenhans'l, R., Eds.; Risø National Laboratory: Roskilde, Denmark, 1995; p 79.

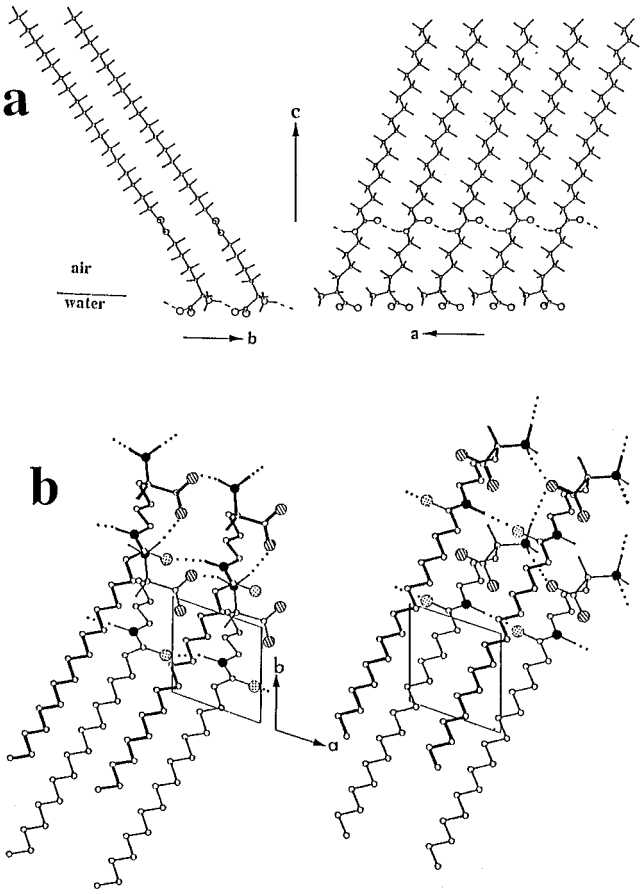

Figure 11. The 2-D crystalline model packing arrangements of the chiral domains, shown for molecules of (*R*) configuration, of the (*R*,*S*)-C_{17}-AM monolayer: Views (a) parallel and (b) perpendicular to the water subphase; in the latter, the two models (*left*, *right*) corresponding to Figure 10. For clarity, the H atoms of the CH_2 and CH_3 groups are omitted and the O and N atoms are shown as filled circles.

crystallographically independent molecules, since both have the same absolute chiral configuration.

Oriented crystallization of α-Glycine by the (*S*)- and (*R*,*S*)-α-Amino Acid Monolayers. The monolayers of enantiomerically pure C_n-AA (n = 10, 12, 16) and C_n-AM (n = 11, 17, 21), when spread over supersaturated glycine aqueous solutions, induced fast crystallization of oriented α-glycine at the interface,[40] in the same way as the natural hydrophobic α-amino acids (*vide supra*). The (*R*) monolayers induced the formation of (010) oriented crystals and the (*S*) monolayers ($0\bar{1}0$) oriented crystals. The degree of (010) or ($0\bar{1}0$) α-glycine orientation by the enantiomerically pure monolayers was, however, lower for C_n-AA than for C_n-AM, presumably due to their lower optical purity.[40] The racemic (*R*,*S*) monolayers yielded fast crystallization of both (010) and ($0\bar{1}0$) oriented α-glycine crystals as did racemic mixture of the water-soluble counterparts (*vide supra*). The C_{29}-AM monolayers, both enantiomerically pure and racemic, were very poor nucleators of α-glycine, consistent with the large mismatch between the packing arrangements of the monolayer head groups and that of the α-glycine layer.

Correlation between Monolayer Crystalline Packing and Oriented Nucleation of α-Glycine. The 2-D crystal structures of all the enantiomerically pure monolayers show that the −HC-(NH_3^+)CO_2^- head groups of the amphiphiles are arranged in a manner similar to the layer structures in the 3-D crystal of α-glycine (Figure 1a) or of the natural hydrophobic α-amino acids. Thus the mechanism of oriented nucleation of α-glycine must first involve binding of glycine solute molecules to the

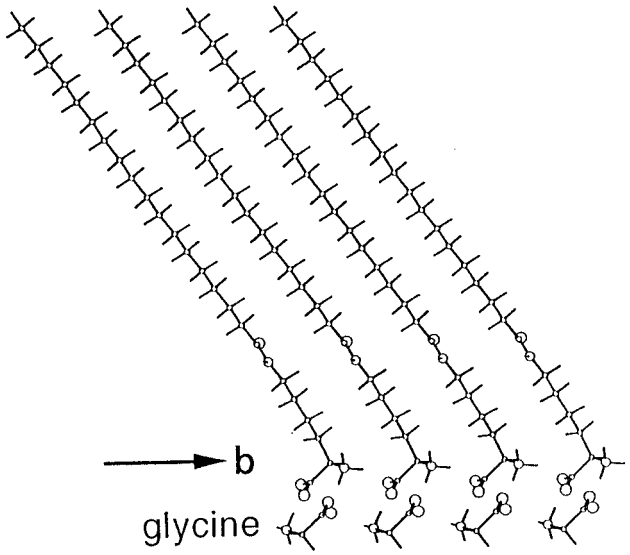

Figure 12. The 2-D crystalline packing arrangement of the chiral domains of the (*S*)-C_{17}-AM monolayer on glycine aqueous solution. View along the *a* axis showing the C_{17}-AM:glycine heterobilayer in which the amphiphile head groups and the underlying glycine molecules are related by a pseudocenter of inversion.

monolayer head groups via *pseudo*inversion symmetry, leading to the formation of a heterobilayer (Figure 12), in a manner similar to that of the bilayer structure in α-glycine (Figure 1b). The glycine molecules of the heterobilayer expose toward the solution C−H bonds oriented approximately normal to the layer. Further attachment of an additional layer of glycine molecules, which would involve C−H···H−C and C−H···O(CO_2^-) contacts as in α-glycine (Figure 1b), must then occur via a pseudo *n*-glide plane parallel to that of the heterobilayer, leading to oriented crystal growth. As a consequence, an (*R*) monolayer must induce the formation of only (010) oriented α-glycine crystals and, by symmetry, an (*S*) monolayer only ($0\bar{1}0$) orientation.

We concluded (*vide supra*) that racemic (*R*,*S*)-C_n-AM, n = 11, 17, 21, monolayers are composed of chiral domains of opposite handedness arising from a spontaneous separation of enantiomers. Since equal amounts of (*R*) and (*S*) enantiomorphous domains are formed from the racemic monolayers, equal amounts of (010) and ($0\bar{1}0$) oriented α-glycine crystals should be nucleated, in keeping with observation.

The (*R*,*S*)-C_n-AA, n = 10, 12, 16, monolayers, on the other hand, self-assemble into crystalline *heterochiral* domains. The question that arises is how to understand the macroscopic appearance of both (010) and ($0\bar{1}0$) oriented crystals of α-glycine from a racemic monolayer arrangement. In the unit cell the (*R*) and (*S*) molecules are related by glide symmetry along the *b* axis (Figure 7), with binding of glycine molecules beneath the (*R*,*S*) monolayer via pseudo 2-fold screw symmetry parallel to the *a* axis (Figure 8). Thus the formed (*R*,*S*)-C_n-AA:glycine heterobilayer should expose toward the solution glycine C-H bonds oriented normal to the layer. There is a reasonable lattice match between such C−H bonds and either of the two chiral layers of α-glycine (layer *1* or *2* in Figure 1b), namely the α-glycine layers exposed by an (010) face or by the enantiomorphous ($0\bar{1}0$) face (see Supporting Information).

On these grounds, the (*R*,*S*)-C_n-AA monolayers, in which the molecules are related by glide symmetry, would induce both (010) and ($0\bar{1}0$) oriented crystals of α-glycine with equal probability, in keeping with observation.

Conclusion

This study shows that, on the water surface, racemic mixtures of α-amino acid amphiphiles form two-dimensional crystalline domains that are (i) racemic compounds, (ii) conglomerates, i.e., a mixture of the enantiomorphous crystals, and perhaps (iii) random solid solutions.

We have demonstrated it is possible to design amphiphilic α-amino acids forming either homochiral or heterochiral crystallites, depending on the nature of the hydrophobic chain residue. The presence of glycine in the aqueous subphase considerably enhances the amount of two-dimensional crystalline material, particularly for the shorter chain amphiphiles such as C_{10}-AA. However, even with glycine in solution, for chains as short as in the amphiphiles C_8-AA and C_6-AA, no GID patterns were observed (see Supporting Information). Nevertheless, the oriented crystallization of α-glycine under the monolayers or with the use of water-soluble α-amino acids as additives does suggest that the latter must form ordered domains on the solution surface.

The racemic α-amino acid amphiphiles with long *n*-alkyl chains C_n-AA pack in the *heterochiral* arrangement, corresponding to class (i), generated via the formation of the commonly observed herring-bone structure. By extrapolation, the water-soluble racemic norleu, met, and α-aminobutyric acid should also form ordered heterochiral two-dimensional domains at the solution surface.

We have achieved a spontaneous separation into *homochiral* crystalline domains of opposite handedness, corresponding to class (ii), for the racemic α-amino acid amphiphiles C_n-AM, $n = 11, 17, 21$, by inducing the molecular translational motif through introduction of an amide group into the chain. The C_n-AM, $n = 29$, monolayers might be considered a system in which a random solid solution is formed.

The 3-D crystals of the water-soluble branched chain α-amino acids leu, isoleu, and val contain chiral layer arrangements. Whether these molecules as additives to glycine aqueous solutions would prefer translational packing to better accommodate their side chains, as opposed to the herring-bone motif, is still not amenable to direct measurement by grazing incidence X-ray diffraction.

Acknowledgment. We thank the Minerva Foundation, Münich Germany, the Israel Academy of Basic Science and Humanity, and the Danish Foundation for Natural Sciences for financial support. We also acknowledge HASYLAB, DESY, Hamburg for beam time.

Supporting Information Available: Two appendices and one figure describing details of (i) the correlation between crystalline packing of the (*R*,*S*)-C_n-AA monolayers and oriented nucleation of α-glycine and (ii) the evaluation of the degree of two-dimensional crystallinity of hydrophobic water-soluble α-amino acids adsorbed at the solution surface (3 pages). See any current masthead page for ordering and Internet access instructions.

JA9613926